

On the Field Dependence of Free Charge Carrier Generation and Recombination in Blends of PCPDTBT/PC₇₀BM: Influence of Solvent Additives

Steve Albrecht,[†] Wolfram Schindler,[‡] Jona Kurpiers,[†] Juliane Kniepert,[†] James C. Blakesley,[†] Ines Dumsch,[§] Sybille Allard,[§] Konstantinos Fostiropoulos,[‡] Ullrich Scherf,[§] and Dieter Neher^{*,†}

[†]Institute of Physics and Astronomy, Soft Matter Physics, Universität Potsdam, D-14476 Potsdam, Germany

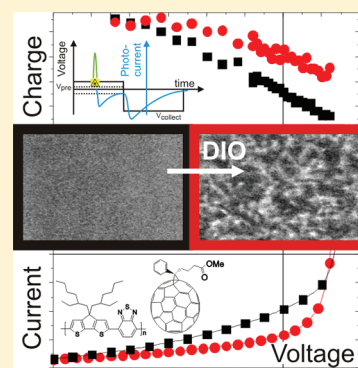
[‡]Helmholtz-Zentrum Berlin für Materialien und Energie, Hahn-Meitner-Platz 1, D-14109 Berlin, Germany

[§]Macromolecular Chemistry and Institute for Polymer Technology, Bergische Universität Wuppertal, Gauss-Strasse 20, D-42097 Wuppertal, Germany

S Supporting Information

ABSTRACT: We have applied time-delayed collection field (TDCF) and charge extraction by linearly increasing voltage (CELIV) to investigate the photogeneration, transport, and recombination of charge carriers in blends composed of PCPDTBT/PC₇₀BM processed with and without the solvent additive diiodooctane. The results suggest that the solvent additive has severe impacts on the elementary processes involved in the photon to collected electron conversion in these blends. First, a pronounced field dependence of the free carrier generation is found for both blends, where the field dependence is stronger without the additive. Second, the fate of charge carriers in both blends can be described with a rather high bimolecular recombination coefficients, which increase with decreasing internal field. Third, the mobility is three to four times higher with the additive. Both blends show a negative field dependence of mobility, which we suggest to cause bias-dependent recombination coefficients.

SECTION: Macromolecules, Soft Matter



The outlook brightens for organic photovoltaics because a dramatic efficiency improvement has been reported over the last 3 years with the introduction of new copolymers as donors in combination with the electron acceptor PCBM.¹ A smart strategy toward higher power conversion efficiencies (PCEs) is to reduce the band gap of the donating polymer by combining electron-rich and electron-deficient units within the conjugated main chain.^{2,3} For some of these polymers, the photovoltaic performance of the resulting bulk heterojunction (BHJ) can be controlled with the help of solvent additives.^{4–7} One of these polymers is poly[2,6-(4,4-bis(2-ethylhexyl)-4H-cyclopenta[2,1-b;3,4-b'']dithiophene)-alt-4,7-(2,1,3-benzothiadiazole)] (PCPDTBT), introduced in 2006 by Konarka Technology Inc.³ For BHJ solar cells composed of PCPDTBT/PC₇₀BM, addition of the processing additive diiodooctane (DIO) was shown to increase the performance by a factor of 2 up to 5.5%.^{6,8} Unfortunately, PCPDTBT/PCBM devices exhibit low fill factors (FFs), implying a strong dependence of the photogenerated current upon internal bias. Though the FF improves considerably upon processing with DIO, it still remains well below the values reported for other high-performance copolymer/fullerene blends.^{2,5,9} Therefore, the main cause of the low FF in PCPDTBT/PCBM blends and the impact of the solvent additive on the elementary processes

involved in the generation and recombination of charges in these blends is the subject of numerous recent publications.^{10–19}

Lenes et al. successfully modeled the current–voltage characteristics of PCPDTBT/PCBM blends (processed without DIO) by considering free carrier generation via field-induced separation of coulombically bound polaron pairs (PPs).²⁰ It was proposed that the low FF in this blend is caused by geminate recombination with a rather short lifetime of the bound pair. It was further proposed that addition of DIO increases this lifetime, from ~500 ns to 3 μs.¹⁷ Field-dependent dissociation of PPs in blends processed without additives was also concluded on the basis of the field-suppressed emission from charge-transfer excitons by Jarzab et al.¹⁵ On the other hand, recent studies with transient absorption spectroscopy (TAS) showed the efficiency for free carrier formation to be independent of the applied bias in PCPDTBT/PC₇₀BM blend devices. The higher short-circuit current in DIO-processed devices was attributed to a higher yield of PP dissociation in conjunction with reduced geminate recombination.¹⁴ An overall more efficient generation of free charges with additive was also revealed by studies of the photoinduced absorption¹⁸ and the

Received: January 20, 2012

Accepted: February 9, 2012

emission of CT states.¹⁹ These observations are in accordance with earlier conclusions by the Konarka group that low FFs in PCPDTBT/PC₇₀BM blends are caused by non-geminate recombination of free carriers rather than by field-dependent split up of bound PPs in competition to geminate recombination.³ Surprisingly, Agostinelli et al. found the bimolecular recombination (BMR) coefficient at identical charge densities to be 6 times higher for blends with the additive, despite the larger FF of these devices.¹⁰ Regarding charge-transport properties, a 4-fold increase of the BIFET mobility of electrons and holes in PCPDTBT/PC₇₀BM processed with DIO was reported.¹¹ On the other hand, dark currents in PCPDTBT/PCBM devices were shown to be unaffected by the additive, implying a very weak impact of the processing conditions on vertical charge transport.¹⁷ In agreement to this, the hole mobility in time-of-flight (TOF) measurements was not significantly altered by the additive.¹⁰

Here, we present studies of the charge carrier dynamics with time-delayed collection field (TDCF)^{21,22} and photo-CELIV measurements in blends of PCPDTBT/PC₇₀BM, processed without and with DIO. In TDCF, carriers are photogenerated with a nanosecond laser pulse at a certain prebias typical for solar cell operation and subsequently extracted with a constant, high reverse bias which is applied after a defined delay time. We optimized our TDCF setup to decrease the minimum delay time to only 10 ns; see the Supporting Information (SI). This allowed us to obtain detailed information on the field dependence of charge carrier generation and recombination with exceptional high temporal resolution. The pulse fluence was chosen to vary between 0.2 and 0.5 $\mu\text{J}/\text{cm}^2$, which yielded a strictly linear dependence of the photogenerated charge carrier density on light intensity (see Figure S2 in SI). The initial photogenerated carrier densities were comparable to steady-state densities under AM 1.5G illumination at 1 sun conditions.²³ Field-dependent mobilities were measured via photo-CELIV²⁴ or deduced from the linear extrapolation of the initial photocurrent decay in the TDCF extraction transients.^{21,25}

Solar cell samples were prepared on structured ITO (Optrex) coated with 60 nm PEDOT/PSS (Clevios AI 4083). The blend solution (1/3 by weight) of PCPDTBT ($M_w = 22300$ g/mol, PDI = 1.31) and PC₇₀BM (Solenne) in chlorobenzene was spincoated with or without 3 vol % DIO, yielding an active layer thickness of 100 nm. The samples were finalized by thermal evaporation of Ca (20 nm) and Al (100 nm) with an active area of 1.1 mm². All samples were encapsulated with epoxy resin and a glass lid prior to air exposure (see SI for details on sample preparation and measurement techniques).

The morphological change induced by the solvent additive DIO was studied with plasmon mapping based on energy-filtered transmission electron microscopy (EFTEM)²⁶ on thin films representative of solar cells (Figure 1). The corresponding energy loss spectra for PCPDTBT, PC₇₀BM, and the blend films (Figure S1 in SI) show that areas with the loss peak at ~ 25 eV (black areas in Figure 1) are rich in PC₇₀BM.²⁶ The morphology without use of DIO is characterized by a highly intermixed small-scale phase separation. Blend layers processed with 3 vol % DIO reveal a higher contrast in the plasmon maps, indicating purer polymer and fullerene phases, with an average domain size of 10–20 nm.

The significant coarsening of the blend morphology with the use of DIO is accompanied by the appearance of a distinct shoulder at 800 nm in the optical absorption spectrum (see Figure S1b, SI). This indicates stronger polymer aggregation

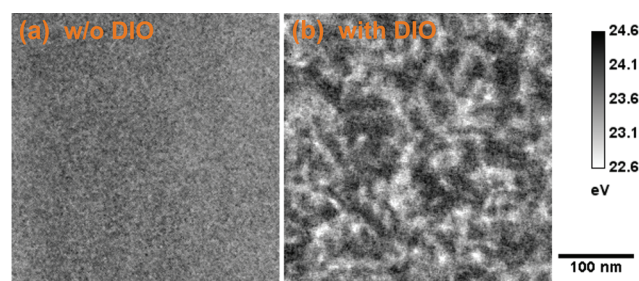


Figure 1. Plasmon maps based on EFTEM images of thin films made of 1/3 blends of PCPDTBT/PC₇₀BM (a) without additive and (b) with 3 vol % DIO. The dark areas refer to PC₇₀BM (see SI).

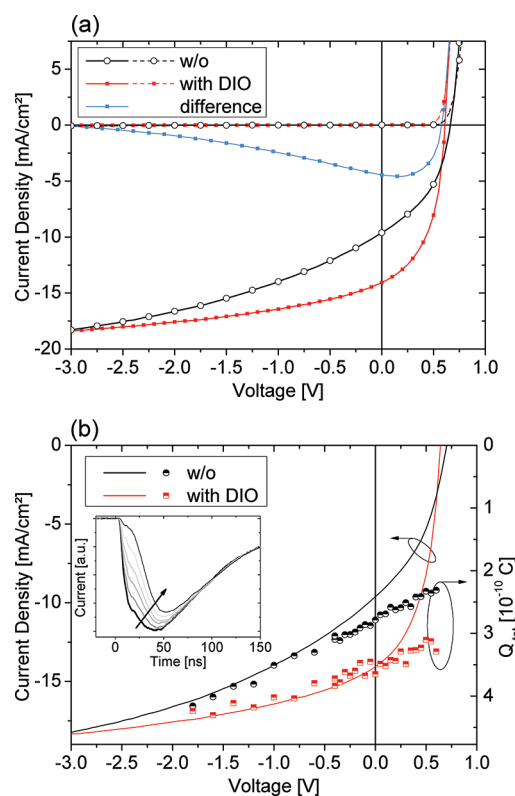


Figure 2. (a) J - V characteristics measured under AM 1.5G at 100 mW/cm^2 from blends of PCPDTBT/PC₇₀BM processed with (red) and without DIO (black). Also shown are the corresponding dark currents (dashed lines + symbols) and the difference in the current under illumination (blue line) between the two blends. (b) Left scale: photocurrent for blends with (red) and without (black) DIO. Right scale: total amount of extracted charge for blends with (red) and without (black) DIO as a function prebias during excitation. Transients were recorded with a delay time of 10 ns and a pulse fluence of 0.2 $\mu\text{J}/\text{cm}^2$. The inset shows the corresponding TDCF transients for blends with additive and V_{pre} ranging from -0.4 to 0.6 V.

and higher intrachain and interchain order within the polymer aggregates.⁶ Note that a higher crystallinity in the PCPDTBT phase of PCPDTBT/PC₇₀BM blend layers processed with DIO has been shown by X-ray diffraction experiments.^{10,27}

Figure 2a shows the solar cell characteristics measured under AM 1.5G at 100 mW/cm^2 and the corresponding dark currents for blends processed without and with DIO. For an active layer thickness of around 100 nm, the performance data without (with) the additive are $J_{\text{sc}} = 9.6$ (13.9) mA/cm^2 , $V_{\text{oc}} = 0.66$ (0.61) V,

FF = 42 (54)%, and PCE = 2.6 (4.5)%. Thus, the main increase in performance stems from the higher J_{sc} and FF. The solid blue line shows the difference between the J - V characteristics under illumination for devices processed with and without the additive. The difference has a maximum at around 0.2 V and vanishes at approximately -3 V, meaning that approximately the same photogenerated charge is collected at the electrodes at high negative bias under AM1.5 illumination.¹⁷

To address a possible field dependence of free carrier formation, we performed TDCF experiments with variable prebias (between -2 and 0.6 V) and a very short delay of 10 ns before application of the collection bias ($V_{coll} = -3$ V). The short delay time was chosen to prevent any losses due to non-geminate recombination prior to the rapid extraction of carriers under the strong collection field. M. A. Loi and co-workers recently studied the steady-state and transient fluorescence properties of PCPDTBT/PC₇₀BM blends processed without the additive. These measurements revealed a bias-independent CT exciton lifetime of 480 ps.¹⁵ Their study also suggested that the formation of such emissive CT excitons proceeds via a weakly bound PP precursor state, which sets the upper limit for the PP lifetime to below 1 ns. This finding was confirmed by recent transient absorption measurements by F. Laquai and co-workers on blends processed with or without additive (unpublished results). These experiments showed a fast subnanosecond decay of strongly bound CT states with lifetimes similar to those reported by M. A. Loi. In addition, blends prepared without the additive displayed a decay component on the time scale of several nanoseconds, which was attributed to the recombination of loosely bound (or spatially trapped) PPs. Therefore, if field-assisted split up of bound PPs is involved in free carrier formation, this process shall be essentially completed before application of the collection bias 10 ns after photoexcitation. In other words, the amount of charge extracted by the electrodes at short t_d and different prebias settings is a direct measure of the field dependence of free carrier formation.

Figure 2b plots the total amount of collected charge Q_{tot} (defined as the integral over the entire current transient) for different values of V_{pre} for devices processed with and without DIO. These measurements were performed with a wavelength of identical absorption for both blends (see Figure S1b, SI). Note that Q_{tot} is the total photogenerated charge that survives geminate and non-geminate recombination and is extracted by the electrodes in the course of the experiment at the specific settings of t_d and V_{pre} .²¹ Two particularities can be attained from these experiments. First, the total extracted charge increases with increasing internal field for both blends, indicative of a field-assisted formation of free charges via bound PPs. This finding is in agreement with results presented by Jarzab et al. showing reduced geminate recombination in PCPDTBT/PCBM blends as the field is increased.¹⁵ Second, the field dependence of generation is stronger for blends without the additive. As a consequence, the efficiency for free carrier generation at short-circuit conditions is substantially larger with the additive, meaning that geminate recombination is suppressed more strongly in the DIO-processed blends. Our finding of a field-dependent efficiency for free carrier formation is at variance with the results from TAS experiments performed in the Durrant group described above. These TAS experiments were performed at a much higher fluence of 8 $\mu\text{J}/\text{cm}^2$, and the probe pulse was delayed by, at minimum, 50 ns. According to our measurements, such high excitation densities lead to severe non-geminate

recombination losses even for very short delay (see, e.g., Figures S2 and S4, SI).

Interestingly, the field dependence of the free charge generation efficiency expressed by Q_{tot} agrees well with the course of the photocurrent characteristics for both blends at negative bias and explains the overall higher steady-state photocurrents of the DIO-processed device (see Figures 2b and S3, SI). At high reverse bias, the free carrier generation efficiency becomes identical for both blends, which is the reason why both photocurrent characteristics merge at negative voltages. Strong derivations are, however, measured when the bias approaches open-circuit conditions, which we attribute to losses by non-geminate recombination. These derivations are more pronounced, and they become obvious at a more negative bias for devices processed without DIO, meaning that non-geminate recombination losses largely determine the photovoltaic properties of these blends at solar cell working conditions.

To address the kinetics of non-geminate recombination, we performed experiments with increasing time delay t_d (in steps of Δt) between the generation and collection of charge carriers. Integration of the transients during delay and during collection yielded the quantities $Q_{pre}(t_d)$ and $Q_{coll}(t_d)$, respectively, with $Q_{tot}(t_d) = Q_{pre}(t_d) + Q_{coll}(t_d)$. Figure 3 shows the

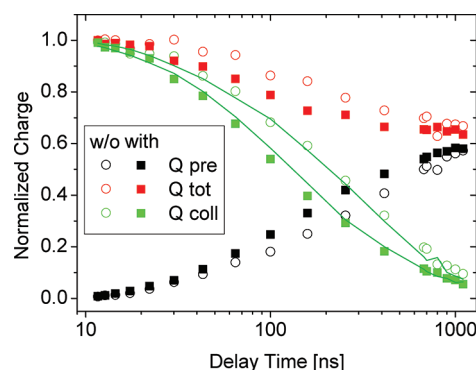


Figure 3. Values for $Q_{pre}(t_d)$, $Q_{coll}(t_d)$, and $Q_{tot}(t_d)$ as determined from TDCF transients recorded for a prebias of 0.3 V as a function of delay time for blends with (filled symbols) and without (open symbols) DIO and corresponding BMR fits (solid lines) according to eq S1 in the SI. The values are normalized to the initially generated charge.

dependence of these quantities as a function of delay time for blends processed without and with the additive for V_{pre} set to 0.3 V. The increase of Q_{pre} with t_d is due to field-induced extraction of photogenerated carriers at pre-bias conditions, leaving less charge available when the collection bias is switched on. Clearly, extraction is more rapid in blends with DIO, leaving fewer charge carriers in the device after a certain delay to recombine. This confirms that the morphology of the blend processed with the additive enables faster extraction of photogenerated charge carriers.

For both blends, a decrease of the total extracted charge is seen already for short delay times of a few tens of nanoseconds, indicating efficient non-geminate recombination. As shown in Figure S4 (SI), a weak decay of Q_{tot} with delay time is observed even for $V_{pre} = 0$ V, meaning that losses due to free carrier recombination cannot be neglected at short-circuit conditions. This is in accordance with the results by Li et al., providing evidence that the photocurrent is hampered by extraction.¹⁶

All data sets of $Q_{pre}(t_d)$ and $Q_{coll}(t_d)$ have been analyzed by an iterative scheme described in the SI to yield the kinetics

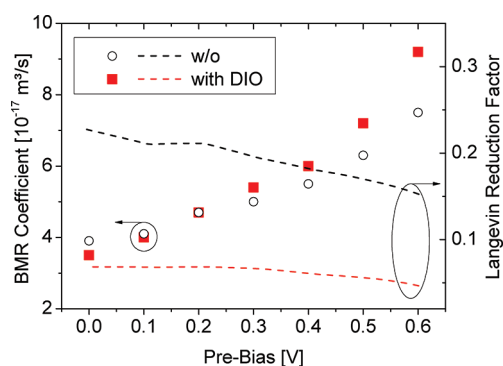


Figure 4. Left scale: BMR coefficient γ_{BMR} for blends with (red filled squares) and without (black open circles) additive, estimated from the fits of TDCF transients with variable delay times between the laser pulse and collection bias to eq S1 (SI) for different prebias. The excitation fluence was $0.5 \mu\text{J}/\text{cm}^2$. The corresponding fits can be found in Figure S4 (SI). Right scale: Langevin reduction factor $\zeta(F)$ for blends with (red dashed line) and without (black dashed line) DIO, estimated from the measured field dependence of mobility.

of non-geminate recombination (see Figure S4 (SI) for further data and fits). Interestingly, excellent fit to the data was possible when assuming BMR. The BMR coefficients γ_{BMR} extracted from these fits are plotted in Figure 4 parameterized in V_{pre} . The values for both blends are rather high, ranging from 3.5 to $9.2 \times 10^{-17} \text{ m}^3/\text{s}$ at short and open circuit, respectively. This is more than 1 order of magnitude higher than BMR coefficients measured with TDCF on the annealed P3HT/PCBM system,²¹ meaning that non-geminate recombination is very fast in the PCPDTBT/PC₇₀BM blend. Interestingly, the absolute value of the coefficient is not altered by the additive. The overall BMR coefficients reported here are higher than those determined by quasi-steady-state TPV measurements when the charge carrier density is set to $5 \times 10^{16} \text{ cm}^{-3}$ for both blends.¹⁰ We assume that initially created “hot” charge carriers have a slightly higher mobility and, therefore, a higher recombination rate compared to that of energetically relaxed charge carriers as measured by TPV.

Notably, the BMR coefficient increases with prebias by a factor of 3 when approaching V_{oc} . As the BMR coefficient is linearly proportional to the drift mobility of electrons and holes, we have determined its field dependence by analyzing photo-CELIV and TDCF transients. The effective field in the photo-CELIV experiments was varied by changing the slope of the voltage ramp, which started $2 \mu\text{s}$ after the laser pulse. Mobilities were determined by the analysis of the photo-CELIV transients according to Bange et al.²⁴ No change in the mobility values was seen when varying the delay time between the laser pulse and voltage ramping between 0.1 and $2 \mu\text{s}$, ruling out a pronounced mobility relaxation at times larger than 100 ns after photo-excitation. For the TDCF measurements, the delay time was set to 100 ns , and the collection voltage was varied from 0.5 to 1.5 V . A lower collection bias caused strong non-geminate recombination during collection, while photocurrent decays at higher biases were limited by the RC time of the setup. Mobility values have been derived from the initial slopes of the photocurrent decays. Flat band was assumed to be at the bias V_0 of zero photocurrent, which is $20\text{--}30 \text{ mV}$ higher than V_{oc} .¹⁷ The so-obtained mobilities are plotted in Figure 5. It was recently shown that the electron mobility in PCPDTBT/PCBM blends is higher than the hole mobility.²⁰ Therefore, we assume that the mobilities shown in Figure 5 correspond to electron

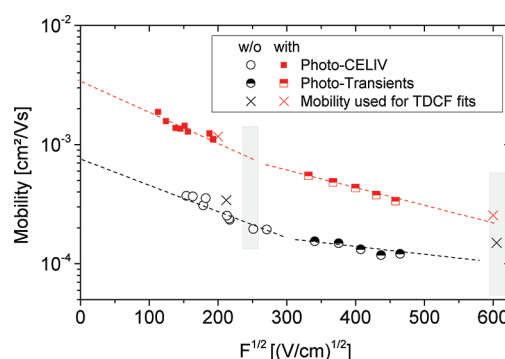


Figure 5. Field-dependent mobilities determined from photo-CELIV (full or open symbols) and TDCF (half-filled symbols) measurements covering a wide range of electrical field on blends processed with (red) or without the additive (black). The dashed lines are guides to the eyes. The gray areas indicate the fields at J_{sc} and extraction at -3 V . The crosses show relaxed electron mobilities at the corresponding fields of 0.2 and -3 V , which gave the best fit to complete TDCF transients with a drift diffusion model in Figure S5 (SI).

mobilities. First, the mobility is seen to be three to four times higher with the additive. Second, both blends show a strong negative dependence on electric field, as is characteristic for materials with high spatial disorder.²⁸ Mobilities with a negative field dependence have occasionally been observed in TOF or CELIV experiments on high mobility materials.^{29,30} Note that space charge limited current (SCLC) measurements on PCPDTBT/PCBM blends processed without the additive were modeled with a mobility that increased with bias (and carrier density).²⁰ These unipolar current measurements analyze the flow of charges injected via ohmic contacts at forward bias in the dark. It has been shown recently that the density of injected carriers at bias voltages larger than V_{oc} might well exceed the photogenerated charge carrier density created under solar cell illumination conditions.³¹ Therefore, mobilities extracted from SCLC measurements should be used with care when interpreting the field dependence of extraction and recombination of photogenerated carriers at voltages below flat band conditions. Drift–diffusion simulations of entire TDCF transients were performed to verify the mobility values and the negative field dependence recorded in our measurements. Exemplary fits are shown in Figure S5 (SI) for a prebias of 0.2 V , a collection bias of -3 V , and four different delay times. Values for the BMR coefficient at the corresponding fields were taken from Figure 5. Best fits were obtained with electron mobilities comparable or slightly higher than the ones plotted in Figure 5 and using hole mobilities that were 2–3 times smaller than the electron mobilities. The fit to the initial rise and decay of the TDCF transients could be considerably improved by considering a modest mobility relaxation^{28,32} within the first 50 ns . The agreement between the simulated and measured transients is excellent, considering that the delay time was varied over a wide range from 10 to 400 ns .

We propose that the negative field dependence of electron and hole mobility is the main cause for the increase in the BMR coefficient with decreasing internal field (increasing device bias). This is demonstrated by the field dependence of the measured Langevin reduction factor $\zeta(F) = \gamma_{\text{BMR}}(F)/\gamma_{\text{L}}(F)$, with $\gamma_{\text{L}} = e(\mu_{\text{e}}(F) + \mu_{\text{h}}(F))/\epsilon_0\epsilon_{\text{r}}$ the Langevin-type three-dimensional recombination coefficient. As shown in Figure 4, $\zeta(F)$ changes only gradually with bias, meaning that the field

dependence of the BMR coefficient is mainly caused by field-dependent mobilities. In the calculation, electron mobilities were taken from Figure S5, and hole mobilities were derived from the TDCF transient fits, with an identical field dependence as that for electrons. Note that $\zeta(F)$ is ~ 3 times lower for devices processed with the additive, meaning that the formation of phase-separated domains of rather pure components slows down BMR.

It was pointed out that a pronounced dependence of the mobility on charge carrier density might cause an increase of the BMR coefficient when approximating open-circuit conditions.²³ With decreasing internal field, the overall carrier density becomes higher due to slower extraction of the photogenerated charge. However, charge-density-dependent mobility measurements with photo-CELIV and cw backlight illumination (data not shown) did not show a significant increase in mobility up to 1 sun illumination conditions in our blends. We also performed TDCF experiments with the pulsed excitation density ranging from 0.2 to 0.5 $\mu\text{J}/\text{cm}^2$. In this range, the BMR coefficient was not significantly altered by the pulsed intensity. We, therefore, conclude that carrier mobilities and, with that, non-geminate recombination coefficients in our PCPDTBT/PCBM blends exhibit an only modest dependence on carrier concentration at solar cell working conditions.

In summary, we have performed measurements of the charge carrier dynamics in solar cells composed of 1:3 blends of PCPDTBT/PC₇₀BM processed with and without the additive DIO utilizing the techniques of TDCF and photo-CELIV. In contrast to the well-known P3HT/PCBM system, we found that the generation of charge carriers is field-dependent in PCPDTBT/PC₇₀BM blends, with the dependence being stronger without the additive. The BMR coefficient increases from 3 to $9 \times 10^{-17} \text{ m}^3/\text{s}$ when the internal field decreases from short- to open-circuit conditions. The coefficient by itself is not altered by the additive when compared at the same bias. Compared to P3HT/PCBM, the BMR coefficient and also the Langevin reduction factor is 1 order of magnitude higher in PCPDTBT/PC₇₀BM blends. The additive speeds up the extraction of charge carriers, which is rationalized by the three-fold increase in mobility in the blends with DIO. Blends processed with and without DIO exhibit a strong negative field dependence of mobility, which is proposed to cause the observed increase in the BMR coefficient when approaching open-circuit conditions. All together, the improvement in charge carrier generation and extraction is identified to cause the two-fold increase in performance when using the additive. The overall moderate performance of the PCPDTBT blends, even when processed with DIO, is proposed to arise from the field-dependent generation of free carriers and the rather high recombination coefficients, which even increase at low internal fields.

■ ASSOCIATED CONTENT

■ Supporting Information

Details on sample fabrication and measurement techniques, electron energy loss spectra, and thin film absorption, Q_{tot} and EQEs from TDCF measurements with different pulse fluences, comparison of ratios (steady-state current versus total extracted charge) between the two blends, Q_{tot} , Q_{pre} , and Q_{coll} for different delay times at 0.0, 0.3, and 0.6 V prebias together with the corresponding BMR fits, and drift diffusion fits to TDCF transients for different delay times. This material is available free of charge via the Internet at <http://pubs.acs.org>.

■ AUTHOR INFORMATION

Corresponding Author

*E-mail: neher@uni-potsdam.de.

Notes

The authors declare no competing financial interest.

■ ACKNOWLEDGMENTS

S.A. acknowledges Marcel Schubert and Sebastian Bange for fruitful discussions. W.S. acknowledges Markus Wollgarten for the cowork with the TEM data. This work was funded by the Bundesministerium für Bildung und Forschung (BMBF) within the PVcomb (FKZ 03IS2151D) and the SOHyb (FKZ 03X3525A) Project.

■ REFERENCES

- (1) Service, R. F. Outlook Brightens for Plastic Solar Cells. *Science* **2011**, 332, 293–293.
- (2) Chu, T.-Y.; Lu, J.; Beaupré, S.; Zhang, Y.; Pouliot, J.-R. m.; Wakim, S.; Zhou, J.; Leclerc, M.; Li, Z.; Ding, J.; et al. Bulk Heterojunction Solar Cells Using Thieno[3,4-*c*]pyrrole-4,6-dione and Dithieno[3,2-*b*:2',3'-*d'*]silole Copolymer with a Power Conversion Efficiency of 7.3%. *J. Am. Chem. Soc.* **2011**, 133, 4250–4253.
- (3) Mühlbacher, D.; Scharber, M.; Morana, M.; Zhu, Z.; Waller, D.; Gaudiana, R.; Brabec, C. High Photovoltaic Performance of a Low-Bandgap Polymer. *Adv. Mater.* **2006**, 18, 2884–2889.
- (4) Amb, C. M.; Chen, S.; Graham, K. R.; Subbiah, J.; Small, C. E.; So, F.; Reynolds, J. R. Dithienogermole As a Fused Electron Donor in Bulk Heterojunction Solar Cells. *J. Am. Chem. Soc.* **2011**, 133, 10062–10065.
- (5) Liang, Y. Y.; Xu, Z.; Xia, J. B.; Tsai, S. T.; Wu, Y.; Li, G.; Ray, C.; Yu, L. P. For the Bright Future-Bulk Heterojunction Polymer Solar Cells with Power Conversion Efficiency of 7.4%. *Adv. Mater.* **2010**, 22, E135–E138.
- (6) Peet, J.; Kim, J. Y.; Coates, N. E.; Ma, W. L.; Moses, D.; Heeger, A. J.; Bazan, G. C. Efficiency Enhancement in Low-Bandgap Polymer Solar Cells by Processing with Alkane Dithiols. *Nat. Mater.* **2007**, 6, 497–500.
- (7) Price, S. C.; Stuart, A. C.; Yang, L.; Zhou, H.; You, W. Fluorine Substituted Conjugated Polymer of Medium Band Gap Yields 7% Efficiency in Polymer–Fullerene Solar Cells. *J. Am. Chem. Soc.* **2011**, 133, 4625–4631.
- (8) Lee, J. K.; Ma, W. L.; Brabec, C. J.; Yuen, J.; Moon, J. S.; Kim, J. Y.; Lee, K.; Bazan, G. C.; Heeger, A. J. Processing Additives for Improved Efficiency from Bulk Heterojunction Solar Cells. *J. Am. Chem. Soc.* **2008**, 130, 3619–3623.
- (9) Sun, Y.; Takacs, C. J.; Cowan, S. R.; Seo, J. H.; Gong, X.; Roy, A.; Heeger, A. J. Efficient, Air-Stable Bulk Heterojunction Polymer Solar Cells Using MoOx as the Anode Interfacial Layer. *Adv. Mater.* **2011**, 23, 2226–2230.
- (10) Agostinelli, T.; Ferenczi, T. A. M.; Pires, E.; Foster, S.; Maurano, A.; Müller, C.; Ballantyne, A.; Hampton, M.; Lilliu, S.; Campoy-Quiles, M.; et al. The Role of Alkane Dithiols in Controlling Polymer Crystallization in Small Band Gap Polymer:Fullerene Solar Cells. *J. Polym. Sci., Part B: Polym. Phys.* **2011**, 49, 717–724.
- (11) Cho, S.; Lee, J. K.; Moon, J. S.; Yuen, J.; Lee, K.; Heeger, A. J. Bulk Heterojunction Bipolar Field-Effect Transistors Processed with Alkane Dithiol. *Org. Electron.* **2008**, 9, 1107–1111.
- (12) Clarke, T.; Ballantyne, A.; Jamieson, F.; Brabec, C.; Nelson, J.; Durrant, J. Transient Absorption Spectroscopy of Charge Photo-generation Yields and Lifetimes in a Low Bandgap Polymer/Fullerene Film. *Chem. Commun.* **2009**, 89–91.
- (13) Hwang, I. W.; Cho, S.; Kim, J. Y.; Lee, K.; Coates, N. E.; Moses, D.; Heeger, A. J. Carrier Generation and Transport in Bulk Heterojunction Films Processed with 1,8-Octanedithiol As a Processing Additive. *J. Appl. Phys.* **2008**, 104, 9.

- (14) Jamieson, F. C.; Agostinelli, T.; Azimi, H.; Nelson, J.; Durrant, J. R. Field-Independent Charge Photogeneration in PCPDTBT/PC(70)BM Solar Cells. *J. Phys. Chem. Lett.* **2010**, *1*, 3306–3310.
- (15) Jarzab, D.; Cordella, F.; Gao, J.; Scharber, M.; Egelhaaf, H.-J.; Loi, M. A. Low-Temperature Behaviour of Charge Transfer Excitons in Narrow-Bandgap Polymer-Based Bulk Heterojunctions. *Adv. Energy Mater.* **2011**, *1*, 604–609.
- (16) Li, Z.; McNeill, C. R. Transient Photocurrent Measurements of PCDTBT:PC(70)BM and PCPDTBT:PC(70)BM Solar Cells: Evidence for Charge Trapping in Efficient Polymer/Fullerene Blends. *J. Appl. Phys.* **2011**, *109*.
- (17) Moet, D. J. D.; Lenes, M.; Morana, M.; Azimi, H.; Brabec, C. J.; Blom, P. W. M. Enhanced Dissociation of Charge-Transfer States in Narrow Band Gap Polymer:Fullerene Solar Cells Processed with 1,8-Octanedithiol. *Appl. Phys. Lett.* **2010**, *96*, 213506.
- (18) Nuzzo, D. D.; Aguirre, A.; Shahid, M.; Gevaerts, V. S.; Meskers, S. C. J.; Janssen, R. A. J. Improved Film Morphology Reduces Charge Carrier Recombination into the Triplet Excited State in a Small Bandgap Polymer-Fullerene Photovoltaic Cell. *Adv. Mater.* **2010**, *22*, 4321–4.
- (19) Scharber, M. C.; Lungenschmied, C.; Egelhaaf, H.-J.; Matt, G.; Bednorz, M.; Fromherz, T.; Gao, J.; Jarzab, D.; Loi, M. A. Charge Transfer Excitons in Low Band Gap Polymer Based Solar Cells and the Role of Processing Additives. *Energy Environ. Sci.* **2011**, *4*, 5077–5083.
- (20) Lenes, M.; Morana, M.; Brabec, C. J.; Blom, P. W. M. Recombination-Limited Photocurrents in Low Bandgap Polymer/Fullerene Solar Cells. *Adv. Funct. Mater.* **2009**, *19*, 1106–1111.
- (21) Kniepert, J.; Schubert, M.; Blakesley, J. C.; Neher, D. Photogeneration and Recombination in P3HT/PCBM Solar Cells Probed by Time-Delayed Collection Field Experiments. *J. Phys. Chem. Lett.* **2011**, *2*, 700–705.
- (22) Popovic, Z. D. A Study of Carrier Generation Mechanism in X-Metal-Free Phthalocyanine. *J. Chem. Phys.* **1983**, *78*, 1552–1558.
- (23) Maurano, A.; Hamilton, R.; Shuttle, C. G.; Ballantyne, A. M.; Nelson, J.; O'Regan, B.; Zhang, W.; McCulloch, I.; Azimi, H.; Morana, M.; et al. Recombination Dynamics as a Key Determinant of Open Circuit Voltage in Organic Bulk Heterojunction Solar Cells: A Comparison of Four Different Donor Polymers. *Adv. Mater.* **2010**, *22*, 4987–4992.
- (24) Bange, S.; Schubert, M.; Neher, D. Charge Mobility Determination by Current Extraction under Linear Increasing Voltages: Case of Nonequilibrium Charges and Field-Dependent Mobilities. *Phys. Rev. B* **2010**, *81*, 035209.
- (25) Cowan, S. R.; Street, R. A.; Cho, S. N.; Heeger, A. J. Transient Photoconductivity in Polymer Bulk Heterojunction Solar Cells: Competition between Sweep-out and Recombination. *Phys. Rev. B* **2011**, *83*, 8.
- (26) Pfannmoeller, M.; Fluegge, H.; Benner, G.; Wacker, I.; Sommer, C.; Hanselmann, M.; Schmale, S.; Schmidt, H.; Hamprecht, F. A.; Rabe, T.; et al. Visualizing a Homogeneous Blend in Bulk Heterojunction Polymer Solar Cells by Analytical Electron Microscopy. *Nano Lett.* **2011**, *11*, 3099–3107.
- (27) Rogers, J. T.; Schmidt, K.; Toney, M. F.; Kramer, E. J.; Bazan, G. C. Structural Order in Bulk Heterojunction Films Prepared with Solvent Additives. *Adv. Mater.* **2011**, *23*, 2284–2288.
- (28) Bäessler, H. Charge Transport in Disordered Organic Photoconductors — A Monte-Carlo Simulation Study. *Phys. Status Solidi B* **1993**, *175*, 15–56.
- (29) Bange, S.; Kuksov, A.; Neher, D.; Vollmer, A.; Koch, N.; Ludemann, A.; Heun, S. the Role of Poly(3,4-Ethylenedioxythiophene):Poly(Styrenesulphonate) As a Hole Injection Layer in a Blue-Emitting Polymer Light-Emitting Diode. *J. Appl. Phys.* **2008**, *104*, 104506.
- (30) Mozer, A. J.; Sariciftci, N. S.; Pivrikas, A.; Osterbacka, R.; Juska, G.; Brassat, L.; Bäessler, H. Charge Carrier Mobility in Regioregular Poly(3-hexylthiophene) Probed by Transient Conductivity Techniques: A Comparative Study. *Phys. Rev. B* **2005**, *71*, 035214.
- (31) Dibb, G. F. A.; Kirchartz, T.; Credgington, D.; Durrant, J. R.; Nelson, J. Analysis of the Relationship between Linearity of Corrected Photocurrent and the Order of Recombination in Organic Solar Cells. *J. Phys. Chem. Lett.* **2011**, *2*, 2407–2411.
- (32) Chen, S.; Choudhury, K. R.; Subbiah, J.; Amb, C. M.; Reynolds, J. R.; So, F. Photo-Carrier Recombination in Polymer Solar Cells Based on P3HT and Silole-Based Copolymer. *Adv. Energy Mater.* **2011**, *1*, 963–969.